searched for shocked quartz (see Fig. 1).

The occurrence of what we interpret to be shocked quartz in several shale beds leads us to suggest that multiple impacts occurred in the latest Triassic, one of which coincided with a locally, and perhaps globally significant extinction at the T-J boundary. The abrupt disappearance of the dominant *Rhaetavicula* fauna immediately below a shale containing shocked quartz, followed by an initially barren zone just above the boundary layer is consistent with the interpretation that the extinction was caused by environmental stresses resulting from an impact event. The lower two shale layers containing shocked quartz are in a part of the section where fossils are scarce (Fig. 1); thus, it is difficult to establish whether there were any faunal changes immediately following deposition of these shales, although Triassic benthic forams are found below and above these two lower shale beds.

Although it is possible that reworking of one impact ejecta layer, or normal fluvial transport from a source region with an older impact structure could account for the occurrence of shocked quartz in three layers, the angularity of the shocked quartz in contrast to the roundness of other sand grains and the occurrence of the shocked quartz in three distinct layers are more consistent with the interpretation of a series of impact events. Studies of the same interval from other sites are required to test the hypothesis of multiple impact events and an associated global extinction at the T-J boundary. Badjukov *et al.* (*28*) reported that shocked quartz was present in multiple levels at the T-J boundary at the Kendelbach section in Austria, but Hallam (*9*) was unable to reproduce this finding.

If the multiple-impact hypothesis is correct, then the events surrounding the T-J boundary would appear to fit the model of a comet shower proposed by Hut *et al.* (*29*), in which a perturbation of the Oort cloud results in multiple impacts over a relatively short period of time; an instantaneous perturbation is expected to produce a number of impacts, 75% of which should occur within the first 0.9 million years. It is difficult to estimate confidently the time spanned by the three shocked quartz-bearing shales, but there are at least 250 m of Norian and Rhaetian beds in the Il Fiume gorge, representing about 15 million years. The resulting average rate of accumulation suggests that the beds A to C may span about 150,000 years, well within the expected time of a comet shower (*29*).

At present, there are no good candidate impact structures for the shocked quartz found in the Corfino section. The Manicouagan impact structure in Quebec has been dated at 214 ± 5 million years ago (Ma) (*30*) and would appear to be unrelated to the T-J boundary on the basis of a recent date of 204 ± 4 Ma for the boundary in the Newark Basin (*31*). Several smaller impact structures have dates that overlap the age for the T-J boundary (*32*), but none can be implicated with any confidence, in consideration of the large errors associated with these ages.


REFERENCES AND NOTES

1. D. M. Raup and J. J. Sepkoski, *Science* **215**, 1501 (1982).
2. ———, *ibid.* **231**, 833 (1986).
3. P. Olsen and H.-D. Sues, in *The Beginning of the Age of the Dinosaurs*, K. Padian, Ed. (Cambridge Univ. Press, Cambridge, 1986), pp. 321–351.
4. P. Olsen, N. H. Shubin, M. H. Anders, *Science* **237**, 1025 (1987).
5. M. J. Benton, *Nature* **321**, 857 (1986).
6. ———, in *Extinction Events in Earth History*, E. G. Kauffman and O. H. Walliser, Eds. (*Lect. Notes Earth Sci. 30*, Springer Verlag, New York, 1990), pp. 239.
7. S. Fowell, *Geol. Soc. Am. Abstr. Progr.* **22**, 355 (1990).
8. A. Hallam, *Paleogeogr. Paleoclimatol. Paleoecol.* **35**, 1 (1981).
9. ———, *Geol. Soc. Am. Spec. Pap.* **247**, 577 (1990).
10. J. J. Sepkoski, *ibid.* **190**, 283 (1982).
11. G. D. Stanley, *Palaios* **3**, 170 (1988).
12. J. Wiedmann, *Biol. Rev.* **48**, 159 (1973).
13. L. W. Alvarez, W. Alvarez, F. Asaro, H. V. Michel, *Science* **208**, 1095 (1980).
14. W. Alvarez *et al.*, *ibid.* **223**, 1135 (1984).
15. W. Alvarez, *Eos* **71**, 1424 (1990).
16. A. R. Hildebrand and W. V. Boynton, *ibid.*, p. 1424.
17. D. J. McLaren, and W. D. Goodfellow, *Annu. Rev. Earth Planet. Sci.* **18**, 123 (1990).
18. G. Ciarapica, S. Cirilli, L. Passeri, *Mem. Soc. Geol. Ital.* **24**, 155 (1982).
19. M. Fazzouli, E. Fois, A. Turi, *Riv. Ital. Paleontol. Strat.* **94**, 561 (1988). This assignment is based on the widespread occurrence of several Hettangian species of the foraminifer *Turrispirillina*.
20. G. Ciarapica and L. Zaninetti, *Rev. Paleobiol.* **1**, 165 (1982). Preliminary foraminiferal identifications were made based on the nomenclature used by Ciarapica and colleagues.
21. G. Ciarapica, S. Cirilli, L. Passeri, E. Tincianti, *ibid.* **6**, 341 (1987).
22. J. S. Alexopoulos, R. A. F. Grieve, P. B. Robertson, *Geology* **16**, 796 (1988).
23. B. F. Bohor, E. E. Foord, P. J. Modreski, D. M. Triplehorn, *Science* **224**, 867 (1984).
24. B. F. Bohor, P. J. Modreski, E. E. Foord, *ibid.* **236**, 705 (1987).
25. G. A. Izett, *Geol. Soc. Am. Spec. Pap.* **249**, 1 (1990).
26. J. S. Alexopoulos, R. A. F. Grieve, P. B. Robertson, *Geology* **17**, 478 (1989).
27. W. V. Engelhardt and W. Bertsch, *Contrib. Mineral. Petrol.* **20**, 203 (1969).
28. D. D. Badjukov, H. Lobitzer, M. A. Nazarov, *Lunar Planet. Sci.* **XVIII**, 38 (1987).
29. P. Hut *et al.*, *Nature* **329**, 118 (1987).
30. B. Jahn, R. J. Floran, C. H. Simmonds, *J. Geophys. Res.* **83**, 2799 (1979).
31. G. R. Dunning and J. P. Hodych, *Geology* **18**, 795 (1990).
32. R. A. F. Grieve, *Annu. Rev. Earth Planet. Sci.* **215**, 245 (1987).


33. Supported by Petroleum Research Fund grant 22784-GB2, the W. Keck Foundation, and the Pew Charitable Trusts (D.M.B., S.M., and P.W.R.), National Science Foundation grant EAR-9016704 (C.R.N. and C.A.M.), and a grant from the Vice President for Research, Syracuse University (C.R.N. and C.A.M.). We thank W. Alvarez, S. Cirilli, G. Ciarapica, M. Fazzuoli, R. A. F. Grieve, A. Hallam, L. Passeri, P. B. Robertson, G. A. Izett, J. L. Macalady, and A. Montanari for help and comments.

24 June 1991; accepted 15 October 1991


# Optically Transparent, Electrically Conductive Composite Medium


S. JIN, T. H. TIEFEL, R. WOLFE, R. C. SHERWOOD, J. J. MOTTINE, JR.



**The development of an optically transparent yet electrically conductive material made with a composite structure having preferentially arranged conductive paths is described. The medium contains many vertically aligned but laterally isolated chains of ferromagnetic spheres dispersed in a sheet of transparent polymer. The sheet material transmits more than 90 percent of the incident light and is highly conductive only in the thickness direction. When suitably modified, the material exhibits on-off electrical switchability at a certain threshold pressure. These characteristics confer potential usefulness for visual communication devices such as write pads or touch-sensitive screens.**


OPTICALLY TRANSPARENT BUT ELECtrically conductive materials are useful for a variety of visual communication, sensor, or electronic device applications. Transparent materials are in general electrical insulators or high-resistivity semiconductors because they have very low mobile charge carriers. Although some composite materials [such as a glass coated with thin transparent metal or indium–tin oxide (ITO) coating] have both transparency and electrical conductivity, they exhibit only planar conductivity along the surface, and that with relatively high electrical resistivity. A transparent medium with high, through-the-thickness conductivity is potentially useful for a variety of device applications such as write


S. Jin, T. H. Tiefel, R. Wolfe, R. C. Sherwood, AT&T Bell Laboratories, Murray Hill, NJ 07974.
J. J. Mottine, Jr., AT&T Technologies, Omaha, NE 68137.

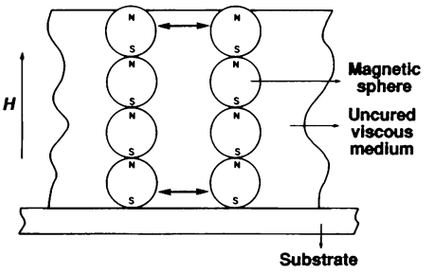


**Fig. 1.** Magnetic poles and interactions of vertical columns of spheres in a viscous medium.

pads, touch-sensitive screens, sensors, and alarm devices. In this report we describe the development of such a medium with desirable optical and electrical characteristics.

In order to create a transparent sheet with vertical conducting paths, we utilized a magnetic field alignment of conductive ferromagnetic particles in a transparent matrix material along the direction of intended light transmission. When ferromagnetic spheres randomly dispersed in a viscous medium are subjected to a unidirectional magnetic field, they move and align themselves into a chain configuration to minimize the magnetostatic energy. Therefore, if a vertical field of suitable intensity is applied to a thin layer of viscous medium containing magnetic particles, parallel, vertically arranged columns (chains of spheres) extending through the thickness of the matrix are formed (*1*). The resultant magnetic dipoles in the neighboring columns (Fig. 1) repel each other, thus positioning the columns toward an equilibrium spacing. The surface tension of the viscous medium prevents the undesirable overgrowth of columns beyond the thickness of the layer. The matrix material (such as glass, silicone elastomer, epoxy resin, and so forth) can then be cured to retain the magnetically aligned conductor structure.

Such a composite structure results in a material that is both optically and electrically anisotropic. The transparency along the vertical ($z$) direction is high (with high transmittance if the density of the columns is kept below a few percent by volume) but is lower in the horizontal ($x$-$y$) direction because of increased light blockage and scattering by the columns. The material is electrically conductive only in the $z$ direction (along the chains of spheres) while insulating in the $x$-$y$ direction. Such anisotropies are useful material characteristics that could be exploited for many device applications.

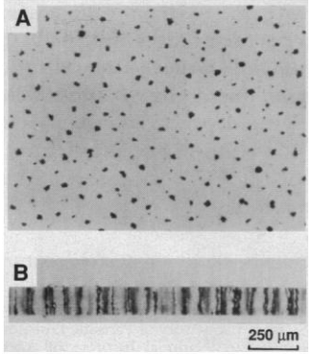


**Fig. 2.** Micrographs showing (**A**) top and (**B**) cross-sectional view of the transparent composite medium.

Approximately 0.5 to 2.0% by volume of Ni spheres with an average diameter of ~20 μm and an Au or Ag coating ~1000 Å thick (for improved conductivity and corrosion resistance) was thoroughly mixed with optically transparent, uncured silicone elastomer (RTV 615, General Electric Company; viscosity, ~40 poises). The mixture was spread on a flat glass substrate and a doctor blade was used to form a thin layer ~150 μm thick; then it was heat-cured (120°C for 15 min) in the presence of a vertical magnetic field of ~600 Oe. The cured sheet was peeled off the substrate and tested for optical and electrical properties.

Shown in Fig. 2 are typical microstructures of the material. Figure 2A reveals that the columns are reasonably well separated and spaced from each other. Most of the columns extend throughout the whole thickness (Fig. 2B). Using a structural model that assumes a perfect triangular arrangement (with sixfold symmetry) of vertical columns, we can estimate the average intercolumnar spacing ($Y$) and the number of columns per unit area ($N$) by the following equations:

$$Y = (D^2/1.65\,x)^{1/2} \quad (1)$$

$$N = 6x/\pi D^2 \quad (2)$$

where $D$ is the particle diameter and $x$ is the volume fraction of the particles in the composite. For $D$ = 20 μm and $x$ = 0.0075, $Y$ is calculated to be ~180 μm and $N$ is ~56 columns per 1.25 by 1.25 mm$^2$ area, which agrees well with the experimental values obtained from the microstructure.

Owing to the vertical arrangement of the particles, the composite material allows easy light transmission along the $z$ direction. Shown in Fig. 3A are the $z$-direction light transmittance and absorbance data in the visible light spectrum (400 to 800 nm) as a function of the volume percent of Ni particles. The transmittance is defined as the intensity ratio of transmitted versus incident light ($I/I_0$ × 100%). The absorbance represents the amount of light absorbed by the medium and is expressed as − log ($I/I_0$). The data have been calibrated against a standard sample containing no Ni particles in order to minimize the effects of surface reflections.

The light transmittance decreases with increasing number of Ni particles (Fig. 3A). About 30% loss in transmittance is observed with a Ni concentration of ~2% by volume (corresponding to approximately 2% in cross-sectional area in the $z$ direction). It is likely that scattering of light caused by the rough top surface and by an altered refractive index in the strained polymer material near the Ni particles is responsible for the loss in transmittance. Indeed, the transmittance is significantly improved if the top surface of the composite is made smoother (from ~70 to ~87% transmittance).

If the volume percent of Ni is kept relatively low, for example, below 0.75%, excellent light transmission (in excess of 90%) is achieved. (The 0.75% Ni sample still provides excellent $z$-direction conductivity with an average through-resistance of less than 1 ohm for 1.25 by 1.25 mm$^2$ area.) Such a high transmittance is essential for clear visibility of underlying word or graphic information in touch-sensitive screen or see-through write pad applications. The light transmittance of the material shows essentially no dependence on wavelength within the visible light range.

For visual communication devices such as touch-sensitive screen or transparent write pad, the light transmission along the off-axis orientations is also important as the screen is often viewed by the user at some angle away from the perpendicular axis. Shown in Fig.

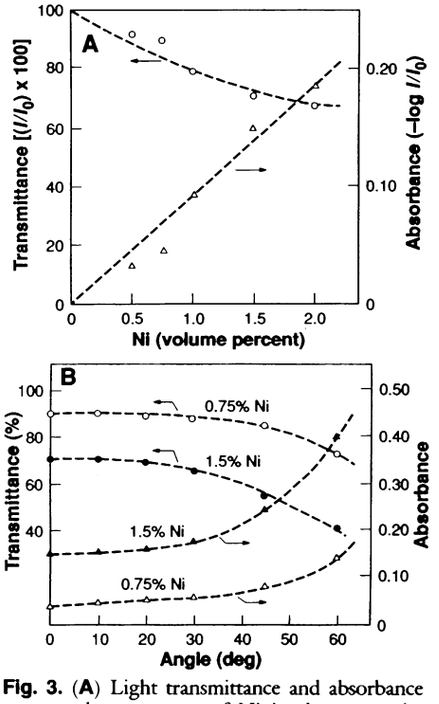


**Fig. 3.** (**A**) Light transmittance and absorbance versus volume percent of Ni in the composite medium. (**B**) Transmittance versus off-axis angle for the composite medium.

3B are the transmittance data as a function of off-axis angle. For the 0.75% Ni sample, the light transmittance remains nearly 90% even at an off-axis angle as much as 30° and decreases only slightly to ~85% at 45° orientation. The angle dependence is slightly more severe in the 1.5% Ni sample (which contains twice as many vertical columns as the 0.75% Ni sample), as might be anticipated from a simple geometrical line-of-sight consideration.

We evaluated the electrical conductivity of the composite medium along the vertical direction (through resistance) by four point resistance measurement, using a constant dc current of 10 mA. The composite sheet was sandwiched between two circuit boards (the lower board contained multiple 1.25-mm-wide conductor lines running in the $x$ direction, whereas the upper board had one 1.25-mm-wide conductor line running in the $y$ direction). A nominal pressure of 5 psi (0.035 MPa) was applied during the measurement to ensure good contacts between the metal spheres. The average through-resistance of the composite medium so measured was ~370 milliohms per 1.25 by 1.25 $mm^2$ contact pad area. For the given sheet thickness of ~150 μm, this resistance value translates into an apparent $z$-direction resistivity of ~0.39 ohm-cm for the composite material. Because there is only 0.75% by volume of the conductor present, the resistivity of the column itself is much lower (~2900 microohm-cm).

The electrical conductivity of the composite medium in the $x$-$y$ direction was measured to be negligible, as might be expected from the microstructure. The in-plane resistivity was $>10^9$ ohm-cm, a value representative of the insulative polymer matrix.

An optically transparent, $z$-direction conductive medium such as described here may be useful as a pressure sensor for visual communication devices such as write pads or finger-touch-sensitive layers on display screens (*2*). The transparency of the pressure sensor is an advantage for tracing an underlying pattern such as a map or chart or for minimizing the loss of display quality underneath a touch-sensitive screen.

In order to make the present composite medium more suitable for transparent write pad type applications, we have further modified the material to achieve electrical on-off switchability. A very thin layer (~5 μm) of silicone elastomer was spray-coated over the top surface of the cured composite material. We have discovered that this extra layer could serve as an insulating barrier at a low applied pressure such as that exerted by a hand resting on the write pad, but it allows $z$-direction electrical conduction above a certain threshold pressure, for example, as exerted by a tip of a writing stylus.

The threshold pressure, which can be adjusted by controlling the barrier thickness, is in the range of 10 to 50 psi (0.069 to 0.345 MPa). Below this threshold, the through-resistance for a 1.25 by 1.25 $mm^2$ pad was greater than 20 megohms, whereas above the threshold the resistance was typically less than ~0.8 ohm. The underlying mechanism for this switchability is not clearly understood. However, it is most likely caused by the upper end of the vertical columns (slightly protruding as shown in Figs. 1 and 2) puncturing through the insulating barrier layer above the threshold pressure and then retracting when the pressure is reduced.

Schematically illustrated in Fig. 4 is an assembly constructed to demonstrate the feasibility of a write pad device that uses the composite medium containing ~1% by volume of the particles. The medium (15 cm by 15 cm by 150 μm) was sandwiched between two Mylar sheets (~75 μm thick) coated with ITO with the conductive side facing the composite medium.

The total electrical resistance was 4827 ohms. It includes the resistance from one edge of the upper ITO layer to the location of the stylus 6 cm away from the edge plus the $z$-direction through-resistance in the composite medium plus the resistance from the stylus to the same-side edge of the lower ITO layer (Fig. 4). (A normal writing pressure by the tip of a pencil is estimated to be ~100 psi, which is over the threshold value of 10 to 50 psi.) Because the through-resistance in the medium contributes not more than ~1 ohm to the combined resistance, the above resistance value represents primarily that of the ITO layers. As the location of the stylus changes, the measured resistance also varies, allowing the $x$-$y$ coordinate positions to be sensed by a number of different schemes (*3, 4*). The total resistance for the case of a hand resting on the pad (~2 psi pressure, well below the threshold) was greater than 20 megohms, thus causing no interference with the position sensing.

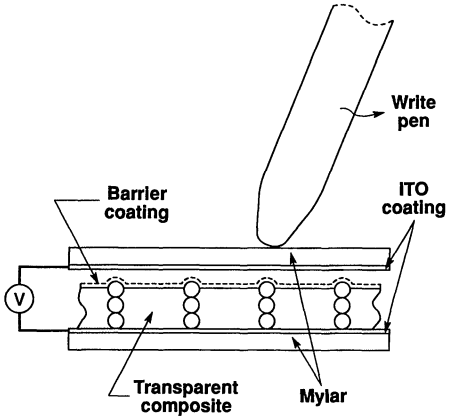


**Fig. 4.** Schematic illustration of an exemplary write pad assembly using the composite medium.


REFERENCES AND NOTES

1. S. Jin *et al.*, *J. Appl. Phys.* **64**, 6008 (1988).
2. S. Jin, J. J. Mottine, R. C. Sherwood, T. H. Tiefel, U.S. Patent 4,664,101 (17 February 1987).
3. D. J. Grover, *Displays* **1** (no. 2), 83 (July 1979).
4. G. J. Ritchie and J. A. Turner, *Int. J. Man-Mach. Stud.* **7**, 639 (1975).


5. We thank G. L. Miller, R. A. Boie, and L. Shepherd for stimulating discussions.

11 September 1991; accepted 13 November 1991


# Sporogonic Development of a Malaria Parasite in Vitro


ALON WARBURG* AND LOUIS H. MILLER



**The sporogonic cycle of the avian malaria parasite *Plasmodium gallinaceum* was completed in vitro. Ookinetes (motile zygotes) were seeded onto a murine basement membrane–like gel (Matrigel) in coculture with *Drosophila melanogaster* cells (Schneider's L2). Transformation into oocysts as well as subsequent growth and differentiation were observed in parasites attached to Matrigel and depended on the presence of L2 cells. Sporozoites were first observed on day 10 in culture. Specific circumsporozoite protein antigenicity was identified in mature oocysts and in sporozoites. It is now possible to follow the entire life cycle of *Plasmodium* in vitro.**


SIGNIFICANT PROGRESS HAS BEEN made in the culture of the intracellular vertebrate stages of malaria parasites. The blood stages of many species multiply readily in continuous culture (*1*), and the exoerythrocytic cycle can also be completed in appropriate cells in vitro (*2*). These achievements stand in marked contrast to the limited success in the cultivation of the


Malaria Section, Laboratory of Parasitic Diseases, Building 4, Room 126, National Institute of Allergy and Infectious Diseases, National Institutes of Health, Bethesda, MD 20892.

*To whom correspondence should be addressed.